Isolation of quenched light-harvesting complex II trimers from *Arabidopsis* leaves with sustained photoprotection (qH)

Pierrick Bru[a,1], Collin J. Steen[b,c,d,1], Soomin Park[b,c,d,1], Cynthia L. Amstutz[e], Emily J. Sylak-Glassman[b,c,d], Michelle Leuenberger[b,c,d], Lam Lam[c,d,f], Fiamma Longoni[g], Graham R. Fleming[b,c,d,f], Krishna K. Niyogi[c,e], Alizée Malnoë[a]*

[a]Umeå Plant Science Centre (UPSC), Department of Plant Physiology, Umeå University, 901 87 Umeå, Sweden
[b]Department of Chemistry, University of California, Berkeley, CA 94720
[c]Molecular Biophysics and Integrated Bioimaging Division, Lawrence Berkeley National Laboratory, Berkeley, CA 94720
[d]Kavli Energy Nanoscience Institute, Berkeley, CA 94720
[e]Howard Hughes Medical Institute, Department of Plant and Microbial Biology, University of California, Berkeley, CA 94720
[f]Graduate Group in Biophysics, University of California, Berkeley, CA 94720
[g]Institute of Biology, University of Neuchâtel, 2000 Neuchâtel, Switzerland

[1]These authors contributed equally to this work

*Correspondence to: alizee.malnoe@umu.se

Keywords: energy dissipation; non-photochemical quenching qH; *Arabidopsis thaliana*; light-harvesting complexes; chlorophyll fluorescence lifetime

Abstract

Excess light can induce photodamage to the photosynthetic machinery, therefore plants have evolved photoprotective mechanisms such as non-photochemical quenching (NPQ). Different NPQ components have been identified and classified based on their relaxation kinetics and molecular players. The NPQ component qE is induced and relaxed rapidly (seconds to minutes), whereas the NPQ component qH is induced and relaxed slowly (hours or longer). Molecular players regulating qH have recently been uncovered, but qH location in the photosynthetic membrane has not been determined. Using time-correlated single-photon counting analysis of the *Arabidopsis thaliana* suppressor of quenching 1 mutant (*soq1*), which displays higher qH than the wild type, we observed shorter average lifetime of chlorophyll fluorescence in leaves and thylakoids relative to wild type. Comparison of isolated photosynthetic complexes from plants in which qH was turned ON or OFF revealed a chlorophyll fluorescence decrease in the trimeric light-harvesting complex II (LHCII) fraction when qH was ON. LHCII trimers are composed of Lhcb1, 2 and 3 proteins, so *lhcb1, lhcb2* and *lhcb3* mutants were crossed with *soq1*. In *soq1 lhcb1*, *soq1 lhcb2*, and *soq1 lhcb3*, qH was not abolished, indicating that no single major Lhcb isoform is necessary for qH. Our work reports the isolation of quenched LHCII directly from plants with active qH, and paves the way for revealing its molecular origin.

Introduction

Photosynthetic organisms possess pigment-protein antenna complexes, which can switch from a light-harvesting state to an energy-dissipating state (Valkunas et al., 2012, Liguori et al., 2015). This switching capability regulates how much light is directed towards photochemistry and ultimately how much carbon dioxide is fixed by photosynthesis (Zhu et al., 2010). The fine-tuning of light energy usage is achieved at the molecular level by proteins which act at or around these pigment-protein complexes (Demmig-Adams et al., 2014). Understanding the regulatory mechanisms involved in the protection against excess light, or photoprotection, has important implications for engineering optimized light-use efficiency in plants, and thereby increasing crop

productivity and/or tolerance to photooxidative stress (Ort et al., 2015, Kromdijk et al., 2016, Wang et al., 2020).

Non-photochemical quenching (NPQ) processes protect photosynthetic organisms by safely dissipating excess absorbed light energy as heat (Horton et al., 1996, Müller et al., 2001). Several NPQ mechanisms have been described and classified based on their recovery kinetics and/or molecular players involved (Malnoë, 2018, Pinnola & Bassi, 2018, Bassi & Dall'Osto, 2021). In plants, the rapidly reversible NPQ, qE, relies on ΔpH, the protein PsbS, and the carotenoid pigment zeaxanthin (Niyogi & Truong, 2013). The slowly reversible NPQ, or sustained energy dissipation, includes several mechanisms such as qZ (zeaxanthin-dependent, ΔpH-independent (Dall'Osto et al., 2005)), qH (see below), and qI (D1 photoinactivation (Krause et al., 1990)). Energy re-distribution can also cause a decrease, i.e. quenching, of chlorophyll (Chl) fluorescence through qT (due to state transition, movement of antenna phosphorylated by the kinase STN7 (Quick & Stitt, 1989)). We have recently uncovered, using chemical mutagenesis and genetic screens in *Arabidopsis thaliana*, several molecular players regulating qH (Brooks et al., 2013, Malnoë et al., 2018, Amstutz et al., 2020, Bru et al., 2020). qH requires the plastid lipocalin, LCNP (Malnoë et al., 2018), is negatively regulated by suppressor of quenching 1, SOQ1 (Brooks et al., 2013), and is turned OFF by relaxation of qH 1, ROQH1 (Amstutz et al., 2020). Importantly, qH is independent of PsbS, ΔpH, xanthophyll pigments and phosphorylation by STN7 (Brooks et al., 2013, Malnoë et al., 2018). Strikingly, when qH is constitutively ON in a *soq1 roqh1* mutant, plants are severely light-limited and display a stunted phenotype (Amstutz et al., 2020). If qH cannot occur (as in an *lcnp* mutant), a higher amount of lipid peroxidation is observed, and plants are severely light-damaged under stress conditions such as cold temperature and high light (Levesque-Tremblay et al., 2009, Malnoë et al., 2018). Our present working hypothesis is that, under stress conditions, LCNP binds or modifies a molecule in the vicinity of or within the antenna proteins, thereby triggering a conformational change that converts antenna proteins from a light-harvesting to a dissipative state.

In wild-type (WT) *Arabidopsis* plants, qH occurs in response to cold and high light (Malnoë et al., 2018), whereas the *soq1* mutant can display qH under non-stress conditions upon a 10-min high light treatment (Brooks et al., 2013). In the double mutant *soq1 chlorina1,* in which the antenna of photosystem II (PSII) does not accumulate, qH is no longer observed, suggesting that

qH occurs in the peripheral antenna of PSII (Malnoë et al., 2018). Here, we aimed to narrow down the location of the qH quenching site within the peripheral antenna of PSII and determine its sensitivity to Lhcb subunit composition. In plants, the peripheral antenna of PSII is composed of pigment-binding, light-harvesting complex (Lhcb) proteins, which are divided into minor subunits (Lhcb4, 5, 6 or CP29, 26, 24, respectively) present as monomers and major subunits (Lhcb1, 2, 3) also referred to as LHCII, forming hetero- and homo-trimeric complexes associated to PSII in a strongly, moderately or loosely bound manner (Ballottari et al., 2012, Crepin & Caffarri, 2018). The pigments associated with the major and minor antenna complexes include Chls *a* and *b*, and carotenoids such as lutein, violaxanthin, zeaxanthin, and neoxanthin (Jahns & Holzwarth, 2012).

We measured the Chl fluorescence lifetimes of intact leaves, isolated thylakoids, and isolated antenna complexes from various *Arabidopsis* mutants relating to qH under non-stress and stress conditions with qH ON or OFF. Due to the sustained nature of qH, we were able to isolate antenna complexes that remained quenched after purification. Isolation of quenched LHCII directly from thylakoid membranes with active qH showed that qH can occur in the major trimeric LHCII complexes. A few studies have reported a quenched conformation of isolated LHCII trimers and in those cases, quenching was achieved in vitro, after full solubilization of LHCII (van Oort et al., 2007, Ilioaia et al., 2008). Through genome editing and genetic crosses, we further demonstrated that qH does not rely on a specific major Lhcb subunit, suggesting that qH is not due to specific amino acid variation among Lhcb1, 2 and 3 (such as phosphorylation in Lhcb1 and 2, or presence of cysteine in Lhcb2.3 or aromatic residues in Lhcb3) and/or that compensation from other major Lhcb proteins may occur.

Results

Fluorescence lifetimes from leaves are shorter with qH ON

We have previously found that the amount of NPQ measured by Chl fluorescence imaging can reach a high level (approximately 12 in the *soq1* mutant) when qH is induced by a cold and high light treatment on whole plants of *Arabidopsis*, but the induction of qH is prevented in a *soq1 lcnp* double mutant (Malnoë et al., 2018). Furthermore, the maximum fluorescence (F_m) from dark-acclimated *soq1 roqh1* plants that display constitutive qH is much lower than control (41 ± 6 in the *soq1 roqh1* mutant vs. 272 ± 8 in wild type), indicating a high NPQ yield, and this quenching does

not occur in a *soq1 roqh1 lcnp* triple mutant (Amstutz et al., 2020). To confirm these findings, we used time-correlated single-photon counting (TCSPC) to measure the fluorescence lifetime from intact leaves (Sylak-Glassman et al., 2016) of *soq1*, *soq1 roqh1 lcnp* (as a negative control that lacks qH), wild type, and *soq1 roqh1*. The amplitude-weighted average fluorescence lifetimes (τ_{avg}) of these first three genotypes were similar in dark-acclimated plants (~1.5 ns, Fig. 1), whereas *soq1 roqh1* displayed a much shorter value (~0.1 ns) consistent with constitutive qH described in (Amstutz et al., 2020).

To induce qH in wild type and *soq1*, we exposed the plants to a 6-h cold and high light treatment. During this treatment, qH is induced and so is qZ as zeaxanthin accumulates (de-epoxidation state value of approximately 0.7 (stress) vs. 0.05 (non-stress) in all lines (Malnoë et al., 2018, Amstutz et al., 2020)); the remaining slowly relaxing quenching processes are grouped under the term qI and are in part due to photoinactivation of PSII. The average fluorescence lifetime of *soq1* cold and high light treated leaves reached similar values as *soq1 roqh1* dark-acclimated leaves (Fig. 1, Fig. S1 and Table S1). Importantly, the calculated NPQτ derived from the τ_{avg} values in *soq1* was approximately 11, which is comparable with the NPQ value measured by video imaging of pulse-amplitude modulated Chl fluorescence. We also observed a lower τ_{avg} value for wild type compared to *soq1 roqh1 lcnp*, consistent with the requirement of LCNP for qH and the induction of qH in wild type by the combination of cold and high light. In agreement with ROQH1 being required for relaxation of qH after a cold and high light treatment, the τ_{avg} of *roqh1* was shorter than wild type (more qH ON) while the lifetime of *soq1 roqh1-1 ROQH1 overexpressor* (OE) was longer than wild type (less qH ON) (Fig. S1). From the τ_{avg} values, NPQτ was calculated (Table S1) and each genotype displayed values that were similar to those found by Chl fluorescence yield measurements (Amstutz et al., 2020). We also further confirmed that qH was independent of PsbS; indeed *soq1 roqh1 npq4* leaves had a low τ_{avg} that was in a similar range, if not lower (~60 ps vs. 130ps), than *soq1 roqh1* (Table S1).

Fluorescence lifetimes from isolated thylakoids are shorter with qH ON

Next, we measured Chl fluorescence lifetimes from isolated thylakoids. Isolated thylakoids from dark-acclimated wild type, *soq1*, and *soq1 roqh1 lcnp* displayed similar τ_{avg} (~1.1 ns, Fig. 2, grey bars), and isolated thylakoids from dark-acclimated *soq1 roqh1* displayed a much lower value (~0.2

ns) consistent with the observations in Fig. 1. Thylakoids were then isolated from plants exposed to a 6-h cold and high light treatment, followed by dark-acclimation for 5 min to relax qE. After a cold and high light treatment, *soq1* also displayed the shortest τ_{avg} of the three lines treated (~0.4 ns vs. ~0.6 ns, Fig. 2), but those values were all higher than what was observed in intact leaves, and the difference in τ_{avg} between wild type and *soq1 roqh1 lcnp* was no longer apparent. The calculated NPQ derived from τ_{avg} was therefore lower than what we observed in intact leaves, but nevertheless the slow relaxation of qH enabled us to measure a difference in NPQτ (2 in *soq1* vs. 0.7 in wild type and *soq1 roqh1 lcnp*) even after the 2 h needed for thylakoid isolation. Release of Chl fluorescence by step solubilization of thylakoid membrane preparation showed that qH depends on incorporation of pigment-protein complexes in the thylakoid (Fig. S2, Q_m *soq1* higher than *soq1 roqh1 lcnp*) and into Chl–protein complexes (Q_{Pi}).

qH is observed in isolated major LHCII

Next, we tested whether we could measure qH from isolated pigment-protein complexes. The lines *soq1* (with qH ON) and *soq1 lcnp* (with qH OFF) were treated with cold and high light (the *roqh1* mutation was omitted as the lack of qH-phenotype remains in either *soq1 roqh1 lcnp* or *soq1 lcnp*), and thylakoids were isolated, solubilized, and fractionated by gel filtration to separate complexes based on their size. The separation profiles of photosynthetic complexes were similar for *soq1* and *soq1 lcnp* (Fig. S3). Fractions corresponding to PSII-LHCII mega-complexes, supercomplexes, PSI-LHCI supercomplexes, PSII core dimer, LHCII trimer, and LHCII/Lhcb monomer as well as smaller fractions (peaks 7, 8) were collected, and their fluorescence yield was measured by video imaging. The LHCII trimer fraction clearly displayed a relatively lower fluorescence value with qH ON (Fig. S4). Room-temperature fluorescence spectra were measured at same low Chl concentration (0.1 μg mL^{-1}) to prevent re-absorption and with excitation at 625 nm (isosbestic point) to excite both Chls *a* and *b* equally; of note Chl *a*/*b* ratio is similar between the compared samples so absorption at 625 nm should be equal. Complexes from non-treated WT were isolated for reference; material came from plants grown under standard light conditions. The LHCII trimer fraction displayed a fluorescence yield at 680 nm that was on average 24% ± 8% lower when qH was ON compared to qH OFF and WT reference (Fig. 3A), whereas the LHCII/Lhcb monomer fraction displayed no significant differences among samples (Fig. 3B, Fig. S5). This result suggests

that qH occurs in the LHCII trimer and can be measured even after isolation of the solubilized protein complex. We confirmed by immunoblot analysis that the protein composition of the compared fractions is similar, namely the LHCII trimer fraction from qH ON and OFF similarly contains a high amount of Lhcb2 and a low amount of Lhcb4 (Fig. S6). We observed a higher content of Lhcb2 in the monomer fractions from the cold and high light treated samples compared to non-treated wild type, which could be due to monomerization of trimers during the cold and high light treatment. A complementary approach separating pigment-protein complexes following solubilization by clear native-PAGE confirmed that qH is active in isolated LHCII trimers (Fig. 4).

Fluorescence lifetimes from isolated LHCII trimer are shorter with qH ON

To further characterize the difference in fluorescence yield observed only from isolated LHCII trimers with qH ON and OFF, we measured their Chl fluorescence lifetimes. Consistent with the ~20% decrease in yield, we observed in the LHCII trimer fraction a ~20% shorter τ_{avg} with qH ON (~2.6 ns ± 0.1 ns, Fig. 5, red bar) vs. qH OFF (~3.3 ns ± 0.2 ns, Fig. 5, blue bar) and no differences in lifetimes in the LHCII/Lhcb monomer and PSII core dimer fractions (red and blue bars). Interestingly, the τ_{avg} of cold and HL-treated LHCII trimer qH OFF was not significantly different from non-treated wild type, and in contrast, the cold and HL-treated LHCII/Lhcb monomer qH ON or OFF displayed shorter lifetimes compared to non-treated wild type. This difference could be attributable to qZ (Dall'Osto et al., 2005) that would be present in the cold and HL-treated samples irrespective of LCNP presence, as both qH ON and OFF monomer samples display the same shorter lifetimes compared to non-treated wild type monomer.

We examined the pigment and protein content by HPLC and SDS-PAGE, respectively, in the LHCII trimer fractions with qH ON or OFF. There were no apparent differences in pigment composition (Fig. S7) or abundance (Fig. S8). This result is in agreement with previous genetic dissection of qH, which did not find involvement of violaxanthin, zeaxanthin, or lutein (Brooks et al., 2013, Malnoë et al., 2018). The protein content was also similar, and there were no visible additional protein bands or size shifts (Fig. S9). Preliminary investigation of possible post-translational modifications of amino acid residues, such as phosphorylation, by protein mass

spectrometry and changes in thylakoid lipids composition by LC-MS in the LHCII trimer fractions with qH ON or OFF indicated no significant differences and will be subject of further work.

qH does not rely on a specific major Lhcb subunit

As a parallel approach to narrow down the antenna site for qH, we used genetic crosses to combine the *soq1* mutation with *lhcb* mutations. The expectation is that the enhanced qH in the *soq1* mutant would no longer be observed if its Lhcb quenching site is absent. We crossed the *soq1* mutant to *lhcb1* and *lhcb2* mutant lines generated by clustered regularly interspaced short palindromic repeat (CRISPR)-CRISPR-associated nuclease 9 (Cas9)-mediated genome editing and to the T-DNA insertional mutant *lhcb3*. The dissection of the Lhcb quenching site is complicated because there are five *LHCB1* and three *LHCB2* genes. However *LHCB1.1, 1.2,* and *1.3* are neighboring genes, as well as *LHCB1.4* and *1.5*, so only three "loci" are segregating upon generating the sextuple mutant *soq1 lhcb1*. The situation is similar for the quadruple *soq1 lhcb2* mutant with three "loci" segregating: *SOQ1*, *LHCB2.1* and *2.2*, and *LHCB2.3*. In addition to genotyping by PCR, lack of specific Lhcb isoforms was confirmed by immunoblot analysis (Fig. S10A). In all three mutant combinations, *soq1 lhcb1*, *soq1 lhcb2*, or *soq1 lhcb3*, additional quenching compared to the respective *lhcb* mutant controls was observed (Fig. 6), which suggests that qH does not require a specific Lhcb isoform. It is important to note that NPQ can be compared between *lhcb* and *soq1 lhcb* mutants as they possess similar F_m values (Fig. 6). In the case of *soq1 lhcb1*, only few trimers are remaining (Pietrzykowska et al., 2014), but the NPQ difference between *lhcb1* and *soq1 lhcb1* is higher than between wild type and *soq1*. We therefore generated the *soq1 lhcb1 lcnp* to ensure that all additional quenching in *soq1 lhcb1* is qH (i.e., LCNP-dependent). The NPQ kinetics of *soq1 lhcb1 lcnp* and *lhcb1* were similar, which confirms that this additional quenching is qH and is enhanced when Lhcb1 is lacking (Fig.6A, S10B).

Discussion

In this paper, we sought to determine the location of qH within the peripheral antenna of PSII and its sensitivity to Lhcb composition. We found that qH does not require a specific Lhcb subunit of LHCII trimers (Fig. 6). Fluorescence lifetimes of isolated trimer fractions indicate that qH likely occurs in the trimeric LHCII (Fig. 5), but the native thylakoid environment is required for its full

extent of quenching (Fig. 1). An alternative explanation could be that qH relaxes slowly during isolation of thylakoids or photosynthetic complexes, or that qH stems from additional energy dissipation routes, not purely at the level of single trimers, such as LHCII aggregation or PSII-PSI spillover, assuming the latter is antenna-dependent or at least Chl *b*-dependent (*soq1 chlorina* no longer displays qH).

Possible additional energy dissipation routes for qH

Miloslavina et al. (Miloslavina et al., 2008) have shown that oligomers or aggregates of LHCII trimers have mixed Chl-Chl excited and charge transfer states emitting in the far-red region of the spectrum and that zeaxanthin is not required but enhances this phenomenon. We have not detected this signal (Fig. S11) and could not fit the decays with a characteristic a fixed lifetime component at 400 ps, as it is too long to fit the fluorescence decays in *soq1 roqh1* displaying constitutive qH with τ_{avg} of 105 or 126 ps (Table S2). This short τ_{avg} value was unchanged whether we selectively excited chlorophyll Chl *a* or *b* (Fig. S12) and was similarly short across detection wavelengths ranging from 640 to 780 nm with shortest lifetime between 660-690 nm, the emission region associated with LHCII, and the PSI emission was shifted towards 720 nm instead of 740 nm when normalized with wild type to their respective maxima (Fig. S11). These results are indicative of a strong LHCII antenna quenching of both PSII-LHCII and possibly PSI-LHCI fluorescence (and/or PSI amount may also be lower). A decay associated spectra analysis was unsuccessful, because we could not simultaneously fit both wild type and *soq1 roqh1* properly (depending on which time component we constrain, it was either too long for *soq1 roqh1* or too short for wild type). A model including τ_{avg} and spectral information could be created (see for a recent example (Bag et al., 2020)) to test whether quenching of PSII is due to energy transfer at PSI (through charge separation from P_{700} or thermal dissipation by P_{700}^{+}), a process referred to as spillover, or quenching at both PSII and PSI is due to thermal dissipation at LHCII. Although we cannot investigate the fluorescence decays as early as ~5 ps due to the longer (30-40 ps) instrument response function (IRF), we observed that the normalized fluorescence decays of wild type and *soq1 roqh1* at 710 nm are almost the same before 100 ps (Fig. S13), suggesting that there is no major contribution of PSII to PSI spillover (within the time-resolution of the IRF).

Less qH in isolated system compared to intact ones

We observed that the average fluorescence lifetimes from thylakoids and isolated trimers are shorter when qH is ON but to a lesser extent than in leaves, and isolated trimers display the least difference among these three types of samples (*soq1*, Fig. 2 and 5 vs. Fig. 1, red bars). It is possible that the qH response observed *in vivo* is due to specific lipid-protein or protein-protein interactions that are altered upon thylakoid extraction and solubilization; comparison of LHCII in detergent micelles vs. membrane nanodiscs shows that quenching is attenuated by detergent (Son et al., 2020). It could also be that qH relaxes slowly during isolation of thylakoids or photosynthetic complexes. The difference in average fluorescence lifetimes could be explained by altered connectivity between the antenna proteins in isolated systems as indicated by the step solubilization of thylakoids (Fig. S2). It has previously been observed that LH1 and LH2 antenna rings in purple bacteria for example displayed a 50% shorter lifetime *in vivo* compared to *in vitro* (Ricci et al., 1996) and similarly that quenching in LHCII was dependent on its membrane environment (Moya et al., 2001, Natali et al., 2016, Saccon et al., 2020, Manna et al., 2021). Lifetimes of pigment-protein complexes largely depend on their local environment, e.g. detergent or proteoliposome (Tietz et al., 2020, Crepin et al., 2021, Nicol & Croce, 2021). The density of the micelles containing the LHCII trimers is similar with qH ON/OFF based on their respective peaks overlaying each other after separation by gel filtration (Fig. S3). It is possible that the trimer fraction contains micelles with one LHCII trimer only and others with one LHCII trimer plus one monomer (consisting of either a major or minor Lhcb). We checked the content of these fractions by immunoblot as a different amount of Lhcb4 could have explained the difference in fluorescence lifetime (Xu et al., 2015) but found that the protein content was similar with qH ON or OFF and specifically that the amount of minor antenna Lhcb4 was similarly low (Fig. S6B and S9). Additionally, we observed quenching in the LHCII trimer by CN-PAGE (Fig. 4) shown to solely contain Lhcb1, 2 and 3 (Rantala et al., 2018b). Furthermore, there could be a mixed population of trimers in an intact leaf, with some having qH ON or OFF, and this would become more evident once isolated (assuming connectivity between trimers is required for full quenching); the resulting average lifetime being an average of an ensemble of LHCII trimers with varying degrees of qH ON and OFF. Using single molecule spectroscopy, we will test whether the LHCII trimer fraction consists of a few trimers highly quenched or all trimers moderately quenched. For qE, it has been

modeled that 12% of sites with active NPQ are sufficient to explain wild-type levels of NPQ (Bennett et al., 2018) and it is feasible that a similar situation could underlie qH.

Location of qH is likely in the LHCII trimer

Decreased fluorescence lifetimes of isolated LHCII trimer fractions with qH ON indicate that qH likely occurs in the trimer (Fig. 4, 5). Through genetic crosses, we found that qH does not require a specific Lhcb subunit of LHCII (Fig. 6), but it may rather require the trimeric conformation as monomerized LHCII and minor antenna proteins have similar fluorescence lifetimes whether qH is ON or OFF (Fig. 5). This interpretation of the results is assuming a similar relaxation rate between the different subcomplexes during isolation. LHCII can form homo-trimers of Lhcb1 or Lhcb2 or hetero-trimers composed of Lhcb1, Lhcb2, and/or Lhcb3 (Standfuss & Kuhlbrandt, 2004); Lhcb1 is the most abundant isoform representing roughly 70% of the total LHCII proteins, whereas Lhcb2 and Lhcb3 abundance is about 20% and 10%, respectively (Standfuss & Kuhlbrandt, 2004). LHCII proteins are highly conserved with an amino acid identity of 82% between Lhcb1 and Lhcb2, 78% between Lhcb1 and Lhcb3, and 79% between Lhcb2 and Lhcb3 (Caffarri et al., 2004). When a specific major Lhcb is missing, other major or minor Lhcb proteins are upregulated and can occupy the place of the missing Lhcb in the trimer, therefore qH may be insensitive to the subunit composition of the trimer. Indeed, when all genes of *LHCB1,* or *LHCB2,* are knocked down, an increase in Lhcb2 and Lhcb3, or Lhcb3 and Lhcb5 respectively, is observed (Pietrzykowska et al., 2014) (however, when all *LHCB1* and *LHCB2* genes are knocked-down, Lhcb5 is not upregulated (Nicol et al., 2019)). Finally, when *LHCB3* is knocked out, an increase of Lhcb1 and Lhcb2 is observed (Damkjaer et al., 2009). Thus, in a major *lhcb* mutant, the antenna complexes are not completely disrupted, and compensation occurs. If qH requires Lhcb trimeric conformation irrespective of its composition, we expect no changes or only slight changes in qH induction in the *soq1 lhcb1*, *2*, or *3* mutants as we have found (Fig. 6). The enhanced qH in *soq1 lhcb1* could be explained by a different antenna organization that would promote qH formation and/or slow down its relaxation.

Here, we have characterized the Chl fluorescence lifetime of intact leaves, thylakoids, and isolated antenna complexes with qH ON or OFF directly from plants. We have observed quenching in all

qH ON samples with a larger extent *in vivo*, highlighting the possible need of a preserved thylakoid membrane macroorganisation for a full qH response and/or the existence of additional quenching sites beyond the LHCII trimers for qH. Of note, the LHCII trimer fraction displayed qH whereas the monomer fraction did not, and qH does not rely on a specific major Lhcb protein. Future work will focus on identifying differences in LHCII trimers that are associated with qH ON and elucidation of the photophysical mechanism(s) of qH.

Materials and Methods

Plant material and growth conditions

Wild-type *Arabidopsis thaliana* and derived mutants studied here are of Col-0 ecotype. Mutants from these respective studies were used (only the *soq1-1* and *lcnp-1* alleles were used except for the *soq1 lhcb1 lcnp* line in which *lcnp* mutation was obtained through genome editing): *soq1* (Brooks et al., 2013), *soq1 lcnp* (Malnoë et al., 2018), *roqh1-1*, *-2*, *-3*, *soq1 roqh1-1*, *-2*, *-3*, *soq1 roqh1 ROQH1 OE*, *soq1 roqh1 lcnp*, *soq1 npq4 roqh1* (Amstutz et al., 2020), *lhcb3* (SALK_036200C) (Xu et al., 2012). For clarity, we refer to the *lhcb1* quintuple mutant affected in all five *LHCB1* genes as "*lhcb1*" (CRISPR-Cas9 edits for *lhcb1.1* (nucleotide insertion (nt) 575_576insA), *lhcb1.2* (nt deletion 575del), *lhcb1.3* (nt insertion 419_420insT), *lhcb1.4* (nt insertion 416_417insT), *lhcb1.5* (large deletion 413_581del)) and to the *lhcb2* triple mutant affected in all three *LHCB2* genes as "*lhcb2"* (*lhcb2.1* (SALK_005774C), CRISPR-Cas9 edits for *lhcb2.2* (nt insertion 10insA), *lhcb2.3* (nt insertion 93insA)). Mutants *soq1 lhcb1*, *soq1 lhcb2, soq1 lhcb3* and *soq1 lhcb1 lcnp* were generated in this study. Plants were grown on soil (Sunshine Mix 4/LA4 potting mix, Sun Gro Horticulture Distribution (Berkeley), 1:3 mixture of Agra-vermiculite "yrkeskvalité K-JORD" provided by RHP and Hasselfors garden respectively (Umeå)) under a 10/14h light/dark photoperiod at 120 µmol photons m^{-2} s^{-1} at 21°C, referred to as standard conditions (Berkeley) or 8/16h at 150 µmol photons m^{-2} s^{-1} at 22 °C/18°C (Umeå) for 5 to 6 weeks or seeds were surface sterilized using 70% ethanol and sown on agar plates (0.5 x Murashige and Skoog (MS) Basal Salt Mixture, Duchefa Biochemie, with pH adjusted to 5.7 with KOH) placed for 1 day in the dark at 4 °C, grown for 3 weeks with 12/12h at 150 µmol photons m^{-2} s^{-1} at 22°C and then transferred to soil. For the cold and high light treatment, plants or detached leaves were placed for 6h at 6°C and at 1500 µmol photons m^{-2} s^{-1} using a custom-designed LED panel built by

JBeamBio with cool white LEDs BXRA-56C1100-B-00 (Farnell). Light bulbs used in growth chambers are cool white (4100K) from Philips (F25T8/TL841 25W) for plants grown on soil and from General Electric (F17T8/SP41 17W) for seedlings grown on agar plates.

Genetic crosses, genome editing and genotyping primers

Genetic crosses were done using standard techniques (Weigel & Glazebrook, 2006). Genome editing assisted by CRISPR-Cas9 was used to generate *lhcb1* and *lhcb2* and following the procedure described in (Ordon et al., 2017, Ordon et al., 2020) for the *soq1 lhcb1 lcnp* line. The mutant background *soq1 lhcb1* was used to generate the *soq1 lhcb1 lcnp* line using four sgRNA targeting *AtLCNP* exon 1 (CTTGTTGAAGTGGCAGCAGG), exon 3 (CTCACGTTACTGTCAGAAGA), exon 4 (TGACATCATAAGGCAACTTG) and exon 5 (TCAGTCACTTCACAGTCCTG) designed using the online tool CHOPCHOP (Labun et al., 2019) and further ranked for efficiency score with E-CRISP (Heigwer et al., 2014) for the two sgRNA targeting *AtLHCB1.1*, *LHCB1.2* and *LHCB1.3* CDS (GAGGACTTGCTTTACCCCGG) and *LHCB1.1*, *LHCB1.3*, *LHCB1.4* and *LHCB1.5* CDS (GGTTCACAGATCTTCAGCGA) and the two sgRNA targeting *LHCB2.2* exon 1 (GGATTGTTGGATAGCTGATG) and *LHCB2.3* exon 1 (GATGCGGCCACCGCCATTGG) in the background of a T-DNA insertional mutant for the *LHCB2.1* gene (SALK_005774C). The two sgRNAs targeting *LHCB1* or *LHCB2* genes were inserted into a binary vector under the control of the U6 promoter using the cloning strategy detailed by (Xing et al., 2014). This binary vector contains also the Cas9 gene under the control of the synthetic EC1 promoter that is expressed only in the egg cells (Durr et al., 2018). To identify *lhcb1* and *lhcb2*, resistant plants were screened by Chl fluorescence for NPQ and photosynthetic acclimation based on (Pietrzykowska et al., 2014), and potential candidates were further confirmed by immunoblot using antibodies against Lhcb1 and Lhcb2. For *soq1 lhcb1 lcnp*, plants were transformed by floral dipping with Agrobacterium GV3101 pSoup containing the vector pDGE277 with the four sgRNAs. Seeds from transformed plants were plated and selected on MS plates with 25 µg mL^{-1} hygromycin. The hygromycin-resistant plants were selected and the absence of LCNP was confirmed by immunoblot using an antibody raised against LCNP. Phire Plant Direct PCR kit was used for genotyping and sequencing with dilution protocol (ThermoFisher Scientific F130); primer list can be found in Table S3.

Chlorophyll fluorescence imaging

Chl fluorescence was measured at room temperature with Walz Imaging-PAM Maxi (Fig. S3, S4) or with SpeedZenII from JbeamBio (Fig. 4, 6). For NPQ measurements, plants or detached leaves were dark-acclimated for 20 min and NPQ was induced by 1200 µmol photons m^{-2} s^{-1} for 10 min and relaxed in the dark for 10 min. Maximum fluorescence after dark acclimation (F_m) and throughout measurement (F_m') were recorded after applying a saturating pulse of light. NPQ was calculated as (F_m-F_m')/F_m'. F_v/F_m is calculated as (F_m-F_o)/F_m where F_o is the minimum fluorescence after dark acclimation.

Thylakoid extraction

Thylakoid extractions were performed according to (Iwai et al., 2015). Briefly, leaves from 6 to 8-week-old plants were ground in a blender for 30 s in 60 mL B1 cold solution (20 mM Tricine-KOH pH7.8, 400 mM NaCl, 2 mM $MgCl_2$). Protease inhibitors are used at all steps (0.2 mM benzamidine, 1 mM aminocaproic acid, 0.2 mM PMSF). The solution is then filtrated through four layers of Miracloth and centrifuged 5 minutes at 27,000 x g at 4°C. The supernatant is discarded, and the pellet is resuspended in 15 mL B2 solution (20 mM Tricine-KOH pH 7.8, 150 mM NaCl, 5 mM $MgCl_2$). The resuspended solution is overlayed onto a 1.3 M/1.8 M sucrose cushion and ultracentrifuged for 30 min in a SW28 rotor at 131,500 x g and 4°C. The band between the sucrose layers is removed and washed with B3 solution (20 mM Tricine-KOH pH 7.8, 15 mM NaCl, 5 mM $MgCl_2$). The solution is centrifuged for 15 min at 27,000 x g and 4°C. The pellet is washed in storing solution (20 mM Tricine-KOH pH 7.8, 0.4 M sucrose, 15 mM NaCl, 5 mM $MgCl_2$) and centrifuged for 10 min at 27,000 x g and 4°C. The pellet is then resuspended in storing solution. Chl concentration is measured according to (Porra et al., 1989). If samples are to be stored, they were flash-frozen in liquid nitrogen and stored at -80°C at approximately 2.5 mg Chl mL^{-1}. Upon using thylakoid preparation, samples are rapidly thawed and buffer is exchanged with 120 mM Tris-HCl pH 6.8, and Chl concentration is measured. For spectroscopy experiments, thylakoids were isolated according to (Gilmore et al., 1998). For the 'before treatment' or 'dark' condition, leaves were detached and dark-acclimated overnight at 4°C.

Isolation of pigment-protein complexes

Thylakoids membranes (400 µg Chl) were solubilized at 2 mg mL^{-1} with 4% (w/v) α-dodecyl maltoside (α-DM) for 15 min on ice (solution was briefly mixed every 5 min), unsolubilized membranes were removed by centrifugation at 14,000 rpm for 5 min. Gel filtration chromatography was performed as described in (Iwai et al., 2015) using the ÄKTAmicro chromatography system with a Superdex 200 Increase 10/300 GL column (GE Healthcare) equilibrated with 20 mM Tris-HCl (pH 8.0), 5 mM $MgCl_2$ and 0.03% (wt/vol) α-DM at room temperature. The flow rate was 1 mL min^{-1}. The proteins were detected at 280 nm absorbance.

Protein analysis

A 5 mm diameter disc was cut from the leaf and frozen into liquid nitrogen. The leaf disc was ground with a plastic pestle and 100 µL of sample loading buffer (62.5 mM Tris pH7.5, 2% SDS, 10% Glycerol, 0.01% Bromophenol blue, 100 mM DTT) was added. Samples were boiled at 95-100°C for 5 min and centrifuged for 3 min. From the samples, 10 µL were loaded onto a 10% SDS-PAGE gel. For the gel filtration fractions, samples were loaded at same volume from pooled adjacent fractions (three fractions for each) onto a 12% SDS-PAGE gel for immunoblot or for silver stain. After migration the proteins were transferred to a PVDF 0.45 µm from ThermoScientific. After transferring the membrane was blocked with TBST+ 3% milk for 1h followed by 1h incubation of the primary antibody (ATPβ AS05 085 (1:5000), LHCB1 AS09 522 (1:5000), LHCB2 AS01 003 (1:10000), LHCB3 AS01 002 (1:2000), LHCB4 AS04 045 (1:7000) from Agrisera and rabbit antibodies against a peptide of LCNP (AEDLEKSETDLEKQ) were produced and purified by peptide affinity by Biogenes and used at a 1:200 dilution) diluted in TBST+ 3% milk. The membrane was washed 3 times 10 min with TBST. Then incubated for 1h with the secondary antibody conjugated to horse radish peroxidase (AS09 602 (1:10000) from Agrisera) in TBST + 3% milk. The membrane was washed 3 times 10 min with TBST and 1 time 5 min with TBS. The Agrisera ECL Bright (AS16 ECL-N-100) and Azure biosystems c600 were used to reveal the bands.

Clear-native PAGE analysis

Thylakoid are washed with the solubilization buffer (25 mM BisTris/HCl (pH 7.0), 20% (w/v) glycerol, 1mM ε-aminocaproic acid and 0.2 mM PMSF) and resuspended in the same buffer at 1

mg Chl mL^{-1}. An equal volume of 2% α-DM was added to the thylakoid solution for 15 min on ice in the dark. Traces of insoluble material were removed by centrifugation at 18,000 x g 20 min 4°C. The Chl concentration was measured, and proteins were loaded at equal Chl content in the native gel (NativePAGE™ 3 to 12%, Bis-Tris, 1.0 mm, Mini Protein Gel, 10-well from ThermoFisher catalog number BN1001BOX). Prior to loading the samples were supplemented with sodium deoxycholate (final concentration 0.3%). The cathode buffer is 50 mM Tricine, 15 mM BisTris, 0.05% sodium deoxycholate and 0.02% α-DM, pH7.0 and anode buffer is 50 mM BisTris, pH7.0. Electrophoresis was performed at 4°C with a gradual increase in voltage: 75 V for 30 min, 100 V for 30 min, 125 V for 30 min, 150 V for 1 h and 175 V until the sample reached the end of the gel. Method adapted from (Rantala et al., 2018a).

Pigment extraction and analysis

HPLC analysis of carotenoids and Chls was done as previously described (Müller-Moulé et al., 2002). 10 µg Chl of fraction samples were extracted in 200 µl 100% acetone.

Fluorescence spectroscopy on isolated thylakoids or complexes

Room temperature fluorescence emission of gel filtration fractions and dependence on step solubilization of thylakoids were performed according to (Dall'Osto et al., 2005) using a Horiba FluoroMax fluorimeter and Starna cells 18/9F-SOG-10 (path length 10mm) with Chl concentration of 0.1 µg mL^{-1}. For the emission spectrum of gel filtration fractions (emission 650 to 800 nm with excitation at 625 nm, bandwidth, 5 nm for excitation, 5 nm for emission), samples were diluted at same absorption (Δ625-750 nm=0.0005) in 20 mM Tris HCl pH8, 5 mM $MgCl_2$ and 0.03% α-DM. For the step solubilization (emission 680 nm with excitation at 440 nm, bandwidth, 5 nm for excitation, 3 nm for emission), thylakoids preparation were diluted in 20 mM Tris HCl pH8, 5 mM $MgCl_2$, and two different detergents were added: first, α-DM at final 0.5% (w/v) concentration from a 10% stock solution, then Triton X-100 at final 5% (w/v) concentration from a 50% stock solution. After each addition, the cuvette was turned upside-down 3 to 5 times for mixing and time for fluorescence level stabilization was allowed.

Fluorescence lifetime measurements and fitting

Method used is adapted for fluorescence lifetime snapshot from (Steen et al., 2020). Time-correlated single photon counting (TCSPC) was performed on detached leaves, isolated thylakoids and gel filtration fractions. Excitation at 420 nm was provided by frequency doubling the 840 nm output of a Ti:sapphire oscillator (Coherent, Mira 900f, 76 MHz). The laser intensity was ~18,000 μmol photons m^{-2} s^{-1}/pulse (~20 pJ/pulse), sufficient to close reaction centers (Sylak-Glassman et al., 2016). Emission was monitored at 680 nm using a MCP PMT detector (Hamamatsu, R3809U). The FWHM of IRF was ~30-40 ps.

It has been shown that a wide range of exponentials can reasonably fit any ensemble fluorescence decay measurement (Bennett et al., 2018), with no easy way to distinguish between the different "models". Therefore to gain a simple, unbiased description of the fluorescence dynamics in each sample, each decay was fit to a tri-exponential model (Picoquant, Fluofit Pro-4.6) without constraining any specific kinetic component, and an amplitude-weighted average fluorescence lifetime (τ_{avg}) was calculated. The extent of quenching was then evaluated by comparison of τ_{avg} values from non-treated (dark) and treated (cold and HL) plants, quantified as $NPQ\tau = \frac{\tau_{avg,\,dark} - \tau_{avg,light}}{\tau_{avg,light}}$. Prior to each measurement, qE was relaxed by dark-acclimation for at least 5 min.

Accession Numbers

Sequence data from this article can be found in the Arabidopsis Genome Initiative under accession numbers At1g29920 (LHCB1.1), At1g29910 (LHCB1.2), At1g29930 (LHCB1.3), At1g56500 (SOQ1), At2g05070 (LHCB2.2), At2g05100 (LHCB2.1), At2g34420 (LHCB1.5), At2g34430 (LHCB1.4), At3g27690 (LHCB2.3), At3g47860 (LCNP), At4g31530 (ROQH1), At5g54270 (LHCB3).

Author Contributions: A.M., K.K.N. and G.R.F. designed research; A.M., S.P., C.J.S., E.J.S.-G., C.L.A., M.L. and L.L. performed biochemical isolation and spectroscopy and analyzed the data; F.L. generated the *lhcb1* and *lhcb2* lines; P.B. performed crosses, genome editing, native gels and analyses of *lhcb* mutant combinations. All of the authors discussed the data, and A.M. wrote the paper with input from P.B., C.J.S., G.R.F and K.K.N.

Acknowledgments

We thank Masakazu Iwai for advice and technical assistance regarding isolation of pigment-protein complexes and for critical reading of the manuscript, Alexandra Lee Fisher for helpful discussions regarding fluorescence lifetimes experiments, Julie Guerreiro for assistance with antenna mutant combination analysis, Jingfang Hao for generation of a new LCNP antibody and Yolande Provot for assistance with isolation of the *soq1 lhcb1 lcnp* line; Roberta Croce, Roberto Bassi and anonymous reviewers for critical discussions. This research (Berkeley) was supported by the Division of Chemical Sciences, Geosciences and Biosciences, Office of Basic Energy Sciences, Office of Science, US Department of Energy (Field Work Proposal 449B). K.K.N. is an investigator of the Howard Hughes Medical Institute. A.M. (Umeå) was supported by European Commission Marie Skłodowska-Curie Actions Individual Fellowship Reintegration Panel (845687). The research performed at Umeå (P.B. and A.M.) was supported by grants to UPSC from the Knut and Alice Wallenberg Foundation (2016.0341 and 2016.0352), the Swedish Governmental Agency for Innovation Systems (2016-00504), by a starting grant to A.M. from the Swedish Research Council Vetenskapsrådet (2018-04150) and by a consortium grant from the Swedish Foundation for Strategic Research (ARC19-0051). The research performed at Neuchâtel (F.L.) was supported by the Swiss National Science Foundation (31003A_179417).

Competing Interest Statement: The authors declare no conflict of interest.

Supplemental Data: Fig.S1 to S13 and Table S1 to S3.

References

Amstutz CL, Fristedt R, Schultink A, Merchant SS, Niyogi KK, Malnoë A (2020) An atypical short-chain dehydrogenase-reductase functions in the relaxation of photoprotective qH in Arabidopsis. *Nat Plants* **6**: 154-166

Bag P, Chukhutsina V, Zhang Z, Paul S, Ivanov AG, Shutova T, Croce R, Holzwarth AR, Jansson S (2020) Direct energy transfer from photosystem II to photosystem I confers winter sustainability in Scots Pine. *Nat Commun* **11**: 6388

Ballottari M, Girardon J, Dall'osto L, Bassi R (2012) Evolution and functional properties of photosystem II light harvesting complexes in eukaryotes. *Biochim Biophys Acta* **1817**: 143-57

Bassi R, Dall'Osto L (2021) Dissipation of Light Energy Absorbed in Excess: The Molecular Mechanisms. *Annu Rev Plant Biol* **72**: 47-76

Bennett DIG, Fleming GR, Amarnath K (2018) Energy-dependent quenching adjusts the excitation diffusion length to regulate photosynthetic light harvesting. *Proc Natl Acad Sci U S A* **115**: E9523-E9531

Brooks MD, Sylak-Glassman EJ, Fleming GR, Niyogi KK (2013) A thioredoxin-like/beta-propeller protein maintains the efficiency of light harvesting in *Arabidopsis*. *Proc Natl Acad Sci USA* **110**: 2733-40

Bru P, Nanda S, Malnoë A (2020) A Genetic Screen to Identify New Molecular Players Involved in Photoprotection qH in Arabidopsis thaliana. *Plants* **9**: 1565

Caffarri S, Croce R, Cattivelli L, Bassi R (2004) A look within LHCII: differential analysis of the Lhcb1-3 complexes building the major trimeric antenna complex of higher-plant photosynthesis. *Biochemistry* **43**: 9467-76

Crepin A, Caffarri S (2018) Functions and Evolution of Lhcb Isoforms Composing LHCII, the Major Light Harvesting Complex of Photosystem II of Green Eukaryotic Organisms. *Curr Protein Pept Sci* **19**: 699-713

Crepin A, Cunill-Semanat E, Kuthanova Trskova E, Belgio E, Kana R (2021) Antenna Protein Clustering In Vitro Unveiled by Fluorescence Correlation Spectroscopy. *Int J Mol Sci* **22**

Dall'Osto L, Caffarri S, Bassi R (2005) A mechanism of nonphotochemical energy dissipation, independent from PsbS, revealed by a conformational change in the antenna protein CP26. *Plant Cell* **17**: 1217-32

Damkjaer JT, Kereiche S, Johnson MP, Kovacs L, Kiss AZ, Boekema EJ, Ruban AV, Horton P, Jansson S (2009) The photosystem II light-harvesting protein Lhcb3 affects the macrostructure of photosystem II and the rate of state transitions in Arabidopsis. *Plant Cell* **21**: 3245-56

Demmig-Adams B, Garab G, Adams III W, Govindjee UoI (2014) Non-photochemical quenching and energy dissipation in plants, algae and cyanobacteria. In Springer

Durr J, Papareddy R, Nakajima K, Gutierrez-Marcos J (2018) Highly efficient heritable targeted deletions of gene clusters and non-coding regulatory regions in Arabidopsis using CRISPR/Cas9. *Sci Rep* **8**: 4443

Gilmore AM, Shinkarev VP, Hazlett TL, Govindjee G (1998) Quantitative analysis of the effects of intrathylakoid pH and xanthophyll cycle pigments on chlorophyll a fluorescence lifetime distributions and intensity in thylakoids. *Biochemistry* **37**: 13582-93

Heigwer F, Kerr G, Boutros M (2014) E-CRISP: fast CRISPR target site identification. *Nat Methods* **11**: 122-3

Horton P, Ruban AV, Walters RG (1996) Regulation of Light Harvesting in Green Plants. *Annu Rev Plant Physiol Plant Mol Biol* **47**: 655-684

Ilioaia C, Johnson MP, Horton P, Ruban AV (2008) Induction of efficient energy dissipation in the isolated light-harvesting complex of Photosystem II in the absence of protein aggregation. *J Biol Chem* **283**: 29505-12

Iwai M, Yokono M, Kono M, Noguchi K, Akimoto S, Nakano A (2015) Light-harvesting complex Lhcb9 confers a green alga-type photosystem I supercomplex to the moss Physcomitrella patens. *Nat Plants* **1**: 14008

Jahns P, Holzwarth AR (2012) The role of the xanthophyll cycle and of lutein in photoprotection of photosystem II. *Biochim Biophys Acta* **1817**: 182-93

Krause GH, Somersalo S, Zumbusch E, Weyers B, Laasch H (1990) On the Mechanism of Photoinhibition in Chloroplasts. Relationship Between Changes in Fluorescence and Activity of Photosystem II. *Journal of Plant Physiology* **136**: 472-479

Kromdijk J, Glowacka K, Leonelli L, Gabilly ST, Iwai M, Niyogi KK, Long SP (2016) Improving photosynthesis and crop productivity by accelerating recovery from photoprotection. *Science* **354**: 857-861
Labun K, Montague TG, Krause M, Torres Cleuren YN, Tjeldnes H, Valen E (2019) CHOPCHOP v3: expanding the CRISPR web toolbox beyond genome editing. *Nucleic Acids Res* **47**: W171-W174
Levesque-Tremblay G, Havaux M, Ouellet F (2009) The chloroplastic lipocalin AtCHL prevents lipid peroxidation and protects *Arabidopsis* against oxidative stress. *Plant J* **60**: 691-702
Liguori N, Periole X, Marrink SJ, Croce R (2015) From light-harvesting to photoprotection: structural basis of the dynamic switch of the major antenna complex of plants (LHCII). *Sci Rep* **5**: 15661
Malnoë A (2018) Photoinhibition or photoprotection of photosynthesis? Update on the (newly termed) sustained quenching component, qH. *Environmental and Experimental Botany* **154**: 123-133
Malnoë A, Schultink A, Shahrasbi S, Rumeau D, Havaux M, Niyogi KK (2018) The Plastid Lipocalin LCNP Is Required for Sustained Photoprotective Energy Dissipation in Arabidopsis. *Plant Cell* **30**: 196-208
Manna P, Davies T, Hoffmann M, Johnson MP, Schlau-Cohen GS (2021) Membrane-dependent heterogeneity of LHCII characterized using single-molecule spectroscopy. *Biophysical Journal* **120**: 3091-3102
Miloslavina Y, Wehner A, Lambrev PH, Wientjes E, Reus M, Garab G, Croce R, Holzwarth AR (2008) Far-red fluorescence: a direct spectroscopic marker for LHCII oligomer formation in non-photochemical quenching. *FEBS Lett* **582**: 3625-31
Moya I, Silvestri M, Vallon O, Cinque G, Bassi R (2001) Time-Resolved Fluorescence Analysis of the Photosystem II Antenna Proteins in Detergent Micelles and Liposomes. *Biochemistry* **40**: 12552-12561
Müller P, Li XP, Niyogi KK (2001) Non-photochemical quenching. A response to excess light energy. *Plant Physiol* **125**: 1558-66
Müller-Moulé P, Conklin PL, Niyogi KK (2002) Ascorbate deficiency can limit violaxanthin de-epoxidase activity *in vivo*. *Plant Physiol* **128**: 970-7
Natali A, Gruber JM, Dietzel L, Stuart MCA, van Grondelle R, Croce R (2016) Light-harvesting Complexes (LHCs) Cluster Spontaneously in Membrane Environment Leading to Shortening of Their Excited State Lifetimes *. *Journal of Biological Chemistry* **291**: 16730-16739
Nicol L, Croce R (2021) The PsbS protein and low pH are necessary and sufficient to induce quenching in the light-harvesting complex of plants LHCII. *Sci Rep* **11**: 7415
Nicol L, Nawrocki WJ, Croce R (2019) Disentangling the sites of non-photochemical quenching in vascular plants. *Nat Plants* **5**: 1177-1183
Niyogi KK, Truong TB (2013) Evolution of flexible non-photochemical quenching mechanisms that regulate light harvesting in oxygenic photosynthesis. *Curr Opin Plant Biol* **16**: 307-14
Ordon J, Bressan M, Kretschmer C, Dall'Osto L, Marillonnet S, Bassi R, Stuttmann J (2020) Optimized Cas9 expression systems for highly efficient Arabidopsis genome editing facilitate isolation of complex alleles in a single generation. *Funct Integr Genomics* **20**: 151-162
Ordon J, Gantner J, Kemna J, Schwalgun L, Reschke M, Streubel J, Boch J, Stuttmann J (2017) Generation of chromosomal deletions in dicotyledonous plants employing a user-friendly genome editing toolkit. *Plant J* **89**: 155-168

Ort DR, Merchant SS, Alric J, Barkan A, Blankenship RE, Bock R, Croce R, Hanson MR, Hibberd JM, Long SP, Moore TA, Moroney J, Niyogi KK, Parry MA, Peralta-Yahya PP, Prince RC, Redding KE, Spalding MH, van Wijk KJ, Vermaas WF et al. (2015) Redesigning photosynthesis to sustainably meet global food and bioenergy demand. *Proc Natl Acad Sci U S A* **112**: 8529-36

Pietrzykowska M, Suorsa M, Semchonok DA, Tikkanen M, Boekema EJ, Aro EM, Jansson S (2014) The light-harvesting chlorophyll a/b binding proteins Lhcb1 and Lhcb2 play complementary roles during state transitions in Arabidopsis. *Plant Cell* **26**: 3646-60

Pinnola A, Bassi R (2018) Molecular mechanisms involved in plant photoprotection. *Biochem Soc Trans* **46**: 467-482

Porra RJ, Thompson WA, Kriedemann PE (1989) Determination of accurate extinction coefficients and simultaneous equations for assaying chlorophylls a and b extracted with four different solvents: verification of the concentration of chlorophyll standards by atomic absorption spectroscopy. *Biochimica et Biophysica Acta (BBA) - Bioenergetics* **975**: 384-394

Quick WP, Stitt M (1989) An examination of factors contributing to non-photochemical quenching of chlorophyll fluorescence in barley leaves. *Biochim Biophys Acta* **977**: 287-296

Rantala M, Paakkarinen V, Aro E-M (2018a) Analysis of Thylakoid Membrane Protein Complexes by Blue Native Gel Electrophoresis. *JoVE*: e58369

Rantala M, Paakkarinen V, Aro E-M (2018b) Separation of Thylakoid Protein Complexes with Two-dimensional Native-PAGE. *Bio-protocol* **8**: e2899

Ricci M, Bradforth SE, Jimenez R, Fleming GR (1996) Internal conversion and energy transfer dynamics of spheroidene in solution and in the LH-1 and LH-2 light-harvesting complexes. *Chemical Physics Letters* **259**: 381-390

Saccon F, Durchan M, Bína D, Duffy CDP, Ruban AV, Polívka T (2020) A Protein Environment-Modulated Energy Dissipation Channel in LHCII Antenna Complex. *iScience* **23**

Son M, Pinnola A, Gordon SC, Bassi R, Schlau-Cohen GS (2020) Observation of dissipative chlorophyll-to-carotenoid energy transfer in light-harvesting complex II in membrane nanodiscs. *Nat Commun* **11**: 1295

Standfuss J, Kuhlbrandt W (2004) The three isoforms of the light-harvesting complex II: spectroscopic features, trimer formation, and functional roles. *J Biol Chem* **279**: 36884-91

Steen CJ, Morris JM, Short AH, Niyogi KK, Fleming GR (2020) Complex Roles of PsbS and Xanthophylls in the Regulation of Nonphotochemical Quenching in Arabidopsis thaliana under Fluctuating Light. *J Phys Chem B* **124**: 10311-10325

Sylak-Glassman EJ, Zaks J, Amarnath K, Leuenberger M, Fleming GR (2016) Characterizing non-photochemical quenching in leaves through fluorescence lifetime snapshots. *Photosynth Res* **127**: 69-76

Tietz S, Leuenberger M, Hohner R, Olson AH, Fleming GR, Kirchhoff H (2020) A proteoliposome-based system reveals how lipids control photosynthetic light harvesting. *J Biol Chem* **295**: 1857-1866

Valkunas L, Chmeliov J, Krüger TPJ, Ilioaia C, van Grondelle R (2012) How Photosynthetic Proteins Switch. *The Journal of Physical Chemistry Letters* **3**: 2779-2784

van Oort B, van Hoek A, Ruban AV, van Amerongen H (2007) Equilibrium between quenched and nonquenched conformations of the major plant light-harvesting complex studied with high-pressure time-resolved fluorescence. *J Phys Chem B* **111**: 7631-7

Wang Y, Burgess SJ, de Becker EM, Long SP (2020) Photosynthesis in the fleeting shadows: an overlooked opportunity for increasing crop productivity? *Plant J* **101**: 874-884
Weigel D, Glazebrook J (2006) Setting Up *Arabidopsis* Crosses. *Cold Spring Harbor Protocols*
Xing HL, Dong L, Wang ZP, Zhang HY, Han CY, Liu B, Wang XC, Chen QJ (2014) A CRISPR/Cas9 toolkit for multiplex genome editing in plants. *BMC Plant Biol* **14**: 327
Xu P, Tian L, Kloz M, Croce R (2015) Molecular insights into zeaxanthin-dependent quenching in higher plants. *Sci Rep* **5**: 13679
Xu Y-H, Liu R, Yan L, Liu Z-Q, Jiang S-C, Shen Y-Y, Wang X-F, Zhang D-P (2012) Light-harvesting chlorophyll a/b-binding proteins are required for stomatal response to abscisic acid in Arabidopsis. *Journal of experimental botany* **63**: 1095-1106
Zhu XG, Long SP, Ort DR (2010) Improving photosynthetic efficiency for greater yield. *Annu Rev Plant Biol* **61**: 235-61

Figures

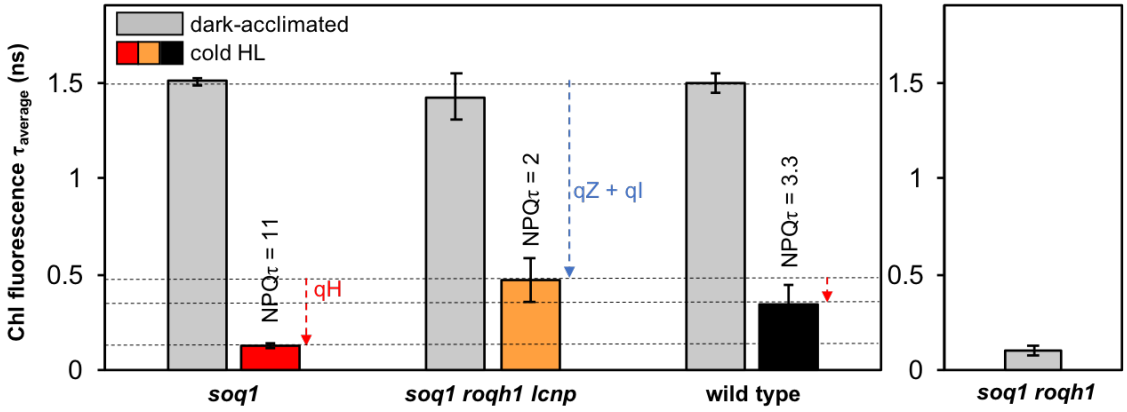

Figure 1. Fluorescence lifetime from leaves are shorter with qH ON.
Average fluorescence lifetime (τ_{avg}) of intact leaves before and after a cold and high-light (cold HL) treatment for 6h which induces qH in wild type and *soq1*. qE is relaxed by dark-acclimating for 5 min before each measurement. NPQτ values are determined based on: NPQτ = $\frac{\tau_{avg,\,dark} - \tau_{avg,light}}{\tau_{avg,light}}$. Data represent means ±SD (n=4 individuals before treatment, n=12 after cold HL treatment and n=17 *soq1 roqh1* no treatment). Excitation at 420 nm and emission at 680 nm.

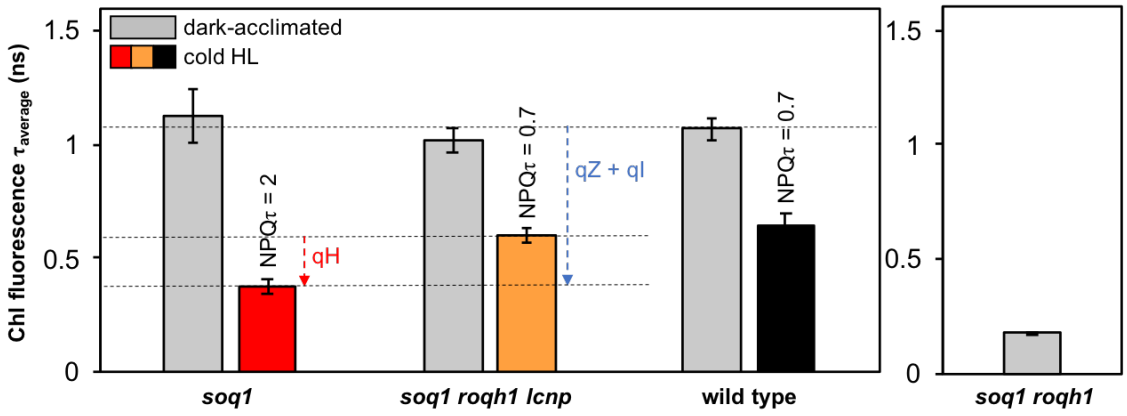

Figure 2. Fluorescence lifetime from isolated thylakoids are shorter with qH ON, but to a lesser extent than in leaves.
Average fluorescence lifetime ($\tau_{average}$) of crude thylakoid membrane isolated before (dark-acclimation overnight) and after a cold and high-light (cold HL) treatment for 6h which induces qH in wild type and *soq1*, qE is relaxed by dark-acclimating for 5 min before thylakoid isolation. Data represent means ±SD (n=3 technical replicates from 2 independent biological experiments).

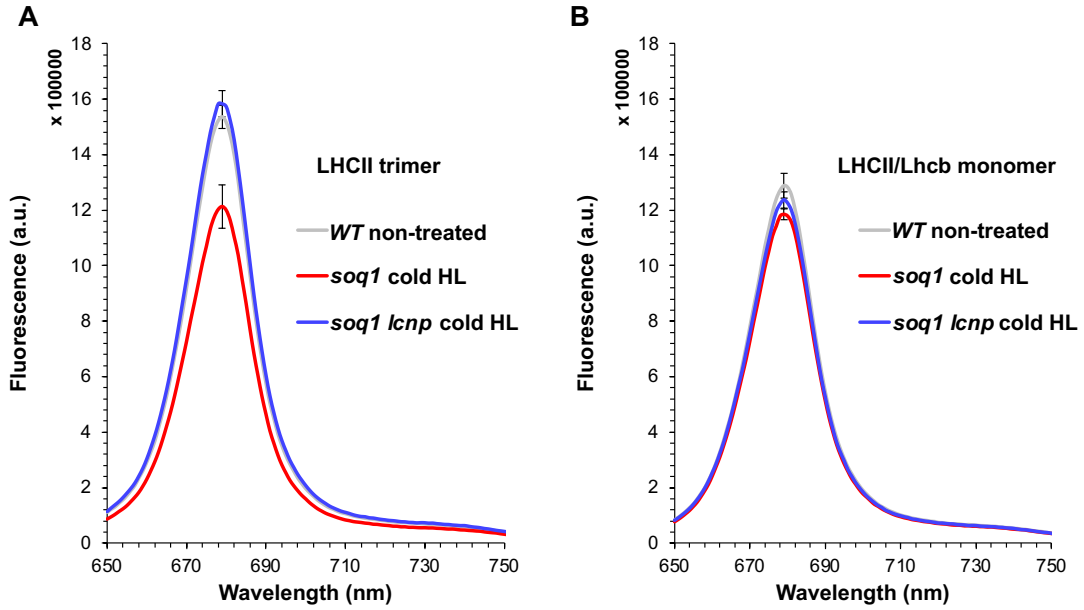

Figure 3. Fluorescence yield is ~24% lower with qH ON in LHCII trimer fraction only. Room temperature fluorescence spectra of isolated LHCII trimer (**A**) and LHCII/Lhcb monomer (**B**) pooled fractions from non-treated wild type (WT) (grey) and cold and HL-treated for 6h40 *soq1* (red) and *soq1 lcnp* (blue) (see Fig. S1 for representative gel filtration experiment and peaks annotation from which fractions were pooled). Fluorescence emission from 650 nm to 750 nm from samples diluted at same chlorophyll concentration (0.1 µg mL^{-1}) with excitation at 625 nm. Data represent means ±SD (n=3 technical replicates). Representative from three independent biological experiments is shown.

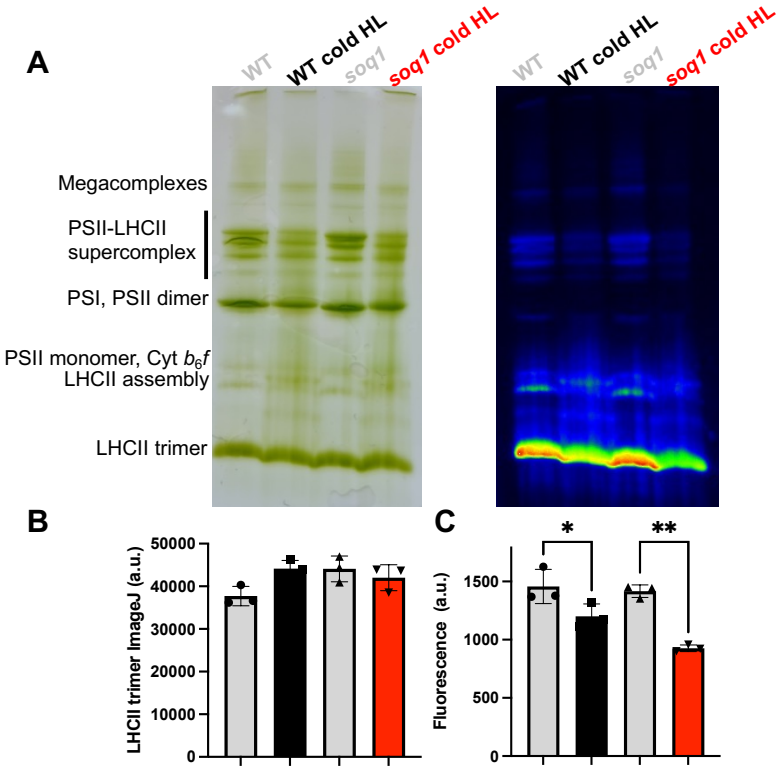

Figure 4. LHCII trimer band displays lower fluorescence when qH ON.
(**A**) Thylakoids were extracted from WT and *soq1* plants (n=3 individuals of each) grown under standard conditions (grey) or cold and high light (cold HL)-treated for 10h (black and red) with NPQ values of respectively 3±1 and 11±1, solubilized in 1% α-DM and separated by clear native PAGE on a 3-12% gel. 10 µg Chl were loaded per lane. Gel image (left) and chlorophyll fluorescence image (right). The composition of the major bands are indicated based on (Rantala *et al.* (2018)). (**B**) Scatter plot with bar representing the quantification of the LHCII trimer band shown in panel A using ImageJ. No statistical difference is measured between the samples. (**C**) Chlorophyll fluorescence quantification of the LHCII trimer band shown in panel A using SpeedZenII software from JBeamBio. Tukey's multiple comparisons test shows a significant decrease in fluorescence level between WT and WT cold HL **P*=0.0450 and between *soq1* and *soq1* cold HL ***P*=0.0011. (**B**,**C)** Data represent means of technical replicates ± SD (n=3 independent loaded gel lanes).

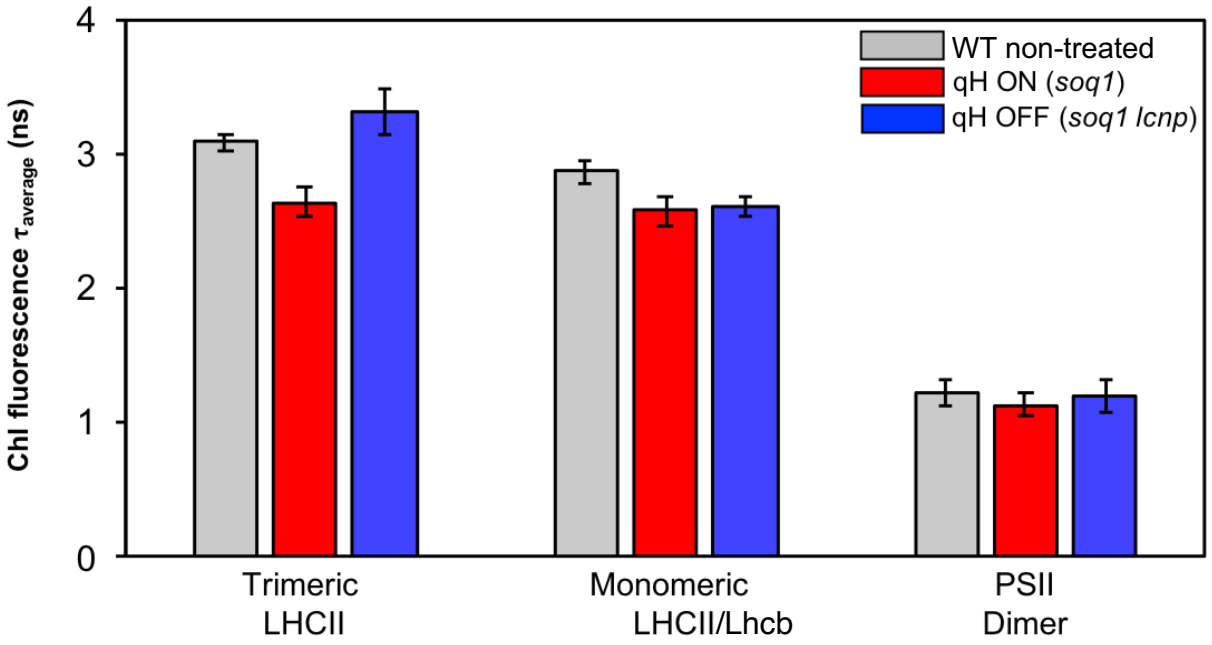

Figure 5. Fluorescence lifetime is 20% lower with qH ON in LHCII trimer fraction only.
Average fluorescence lifetime (τ_{avg}) of trimeric LHCII, monomeric LHCII/Lhcb, and PSII dimer isolated from non-treated wild type (WT) (grey) and cold HL-treated *soq1* (red) and *soq1 lcnp* (blue). Data represent means ±SD (n=3 technical replicates from 2 independent biological experiments).

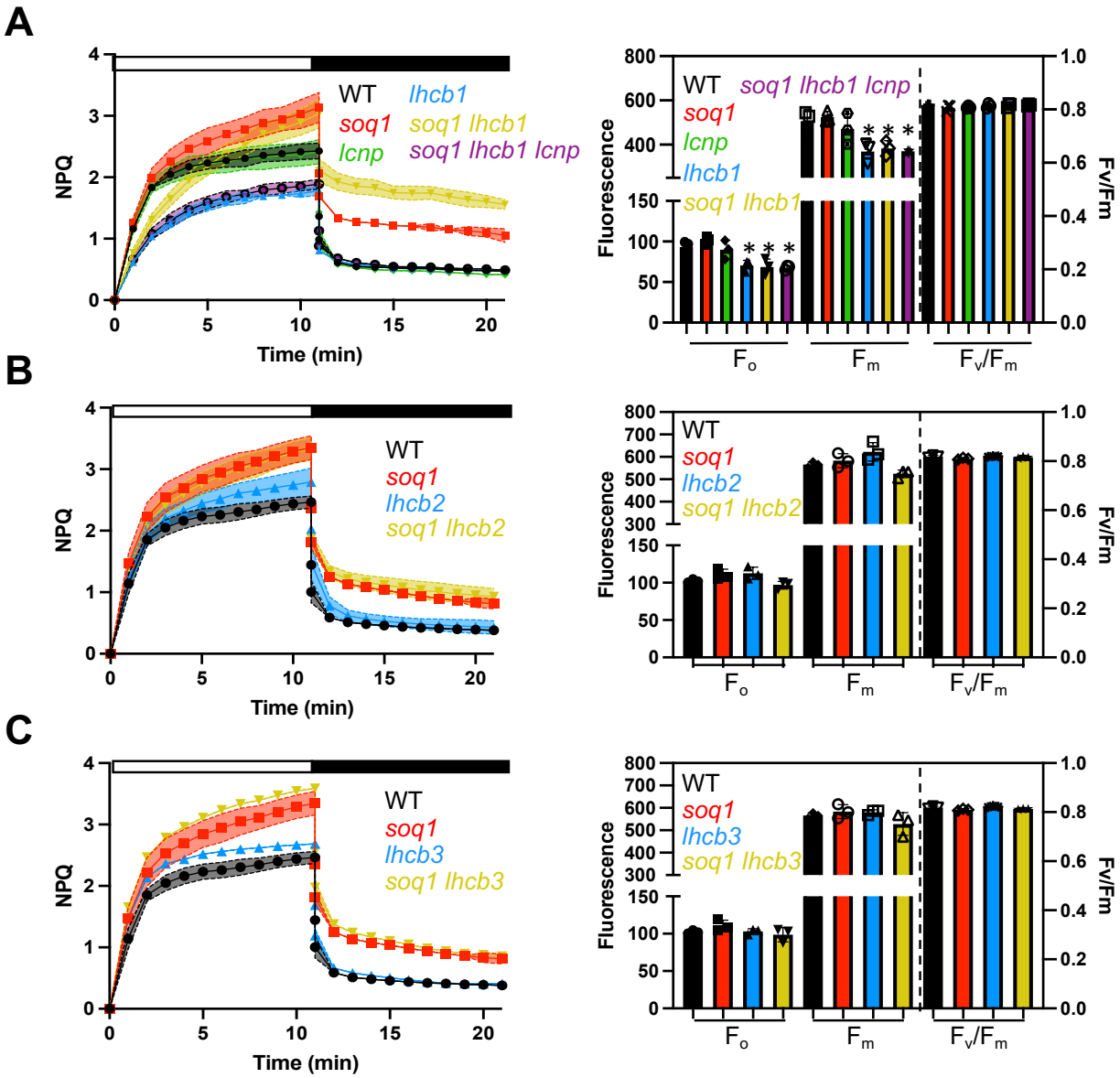

Figure 6. qH does not rely on a specific major Lhcb.
Left panel, NPQ kinetics of dark-acclimated (20 min) WT, *soq1*, (**A**) *lcnp*, *lhcb1*, *soq1 lhcb1* and *soq1 lhcb1 lcnp,* (**B**) *lhcb2* and *soq1 lhcb2,* (**C**) *lhcb3* and *soq1 lhcb3* four-week-old plants grown at 120 µmol photons m^{-2} s^{-1}. Induction of NPQ at 1300 µmol photons m^{-2} s^{-1} (white bar) and relaxation in the dark (black bar). Right panel, photosynthetic parameters F_o, F_m and F_v/F_m of the same plants. Tukey's multiple comparisons test shows that *lhcb1*, *soq1 lhcb1* and *soq1 lhcb1 lcnp* are statistically different from WT for F_o (*P=0.0359, P*=0.0222 and *P*=0.0171, respectively) and F_m (*P*=0.0245, *P*=0.0482 and *P*=0.0257, respectively). Small significant difference in F_m with *P=0.0111* for *lhcb2* and *soq1 lhcb2* was not observed in two other biological replicates. Data represent means ± SD (*n*=3 individuals).